

Low Fe(II) concentrations catalyze the dissolution of various Fe(III) (hydr)oxide minerals in the presence of diverse ligands and over a broad pH range

Kyounglim Kang^a, Walter D.C. Schenkeveld^{a*}[†], Jagannath Biswakarma^{b,c}, Susan C. Borowski^{b‡}, Stephan J. Hug^b, Janet G. Hering^{b,c,d}, Stephan M. Kraemer^{a*}.

^a Department of Environmental Geosciences, University of Vienna, Althanstrasse 14(UZA II) 1090 Vienna, Austria.

^b EAWAG, Swiss Federal Institute of Aquatic Science and Technology, Ueberlandstr. 133, CH-8600, Dübendorf, Switzerland

^c Swiss Federal Institute of Technology (ETH) Zürich, IBP, CH-8092 Zürich, Switzerland

^d Swiss Federal Institute of Technology Lausanne (EPFL), ENAC, CH-1015 Lausanne, Switzerland

[†] Current address: W.D.C. Schenkeveld, Copernicus Institute, Faculty of Geosciences, Utrecht University, Princetonlaan 8A, 3584 CB Utrecht, the Netherlands

[‡]Current address: S.C. Borowski, Virginia Military Institute, Lexington, VA 24450, USA.

*E-mail: w.d.c.schenkeveld@uu.nl; stephan.kraemer@univie.ac.at

Supporting Information

16 Pages

7 Figures

4 Tables

Figure. S1. Adsorption isotherms for Fe(II) onto various Fe(III) (hydr)oxide minerals

Figure. S2. Adsorption isotherms for DFOB and HBED onto various Fe(III) (hydr) oxide minerals in the presence and absence of Fe(II)

Figure. S3. Adsorption isotherms for FeDFOB and FeHBED onto lepidocrocite and goethite in the presence and absence of Fe(II)

Figure. S4. Calculation of dissolution rates

Figure. S5. Calculation of adsorbed Fe(II) concentration at t=0

Figure. S6. Rate coefficients of ligand-controlled dissolution (k_{HBED}) and Fe(II) catalyzed ligand-controlled dissolution ($k_{Fe(II)}HBED$) of each Fe(III) (hydr)oxides.

Figure. S7. XRD patterns of synthesized Fe(III) (hydr)oxides

Table. S1. Materials

Table. S2. Summary of batch experiments and dissolution rates

Table. S3. Modelling results for Fe(II) equilibrium speciation in the presence of DFOB as a function of pH

Table. S4. Effect of pH on the catalytic effect of Fe(II) on ligand controlled dissolution

Figure. S1. Adsorption isotherms for Fe(II) onto various Fe(III) (hydr)oxide minerals (2.5 g L⁻¹ at pH 4 and 6, 0.5 g L⁻¹ at pH 7 and 8.5, 0.01 NaCl). Adsorption data was obtained for different Fe(II) concentration ranges: (a)-(b) 0.5 to 20 µM at pH 4 and 6, 0.5 to 100 µM at pH 7 and 8.5 for lepidocrocite, (c) 0.5 to 20 µM goethite-1, (d) 0.5 to 10 µM for goethite-2 and (e) hematite, and (f) 0.5 to 25 µM for 2-line ferrihydrite. The equilibration time was 30 minutes. Q_{max} and K_D values were calculated based on the Langmuir model (blue line).

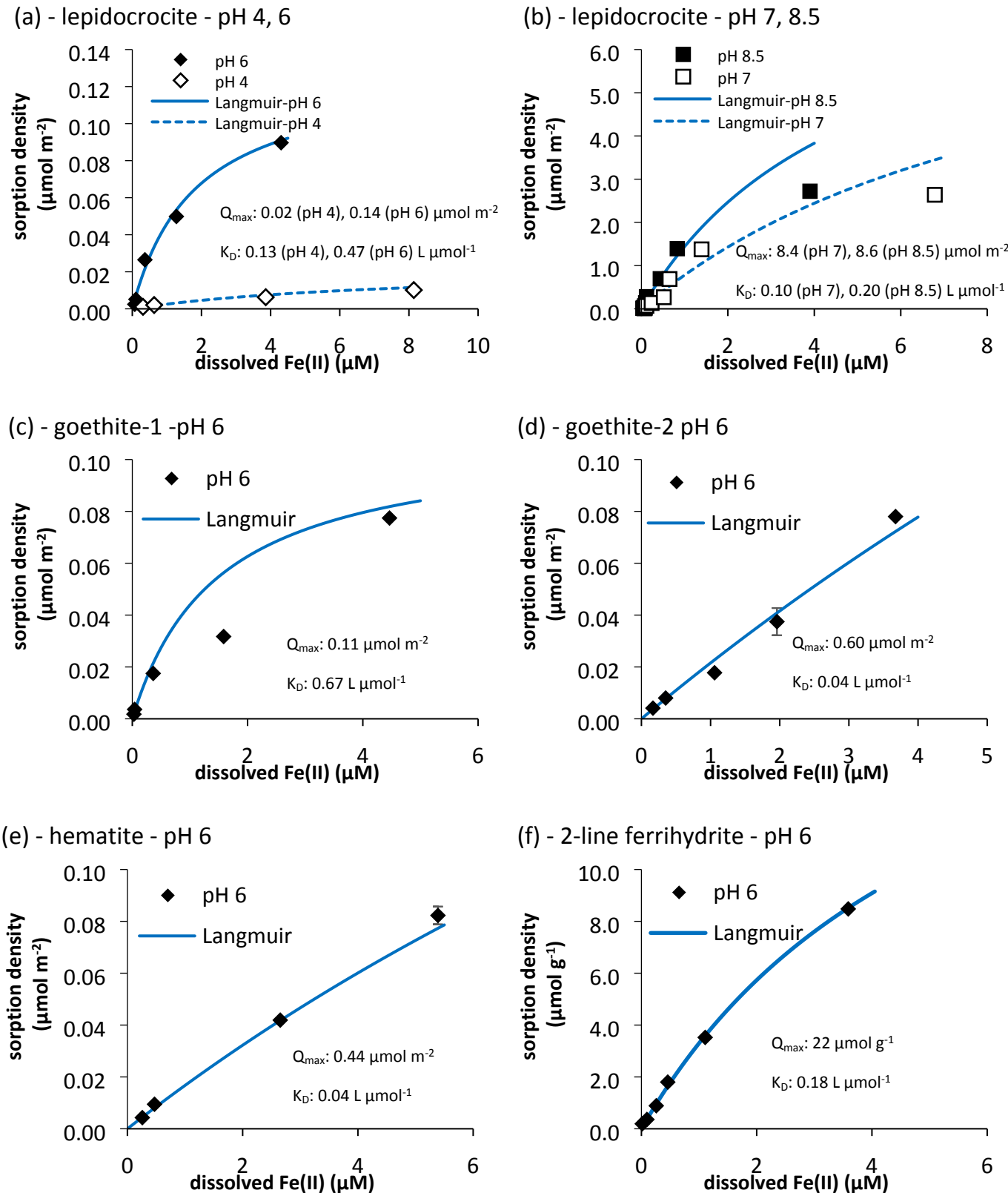
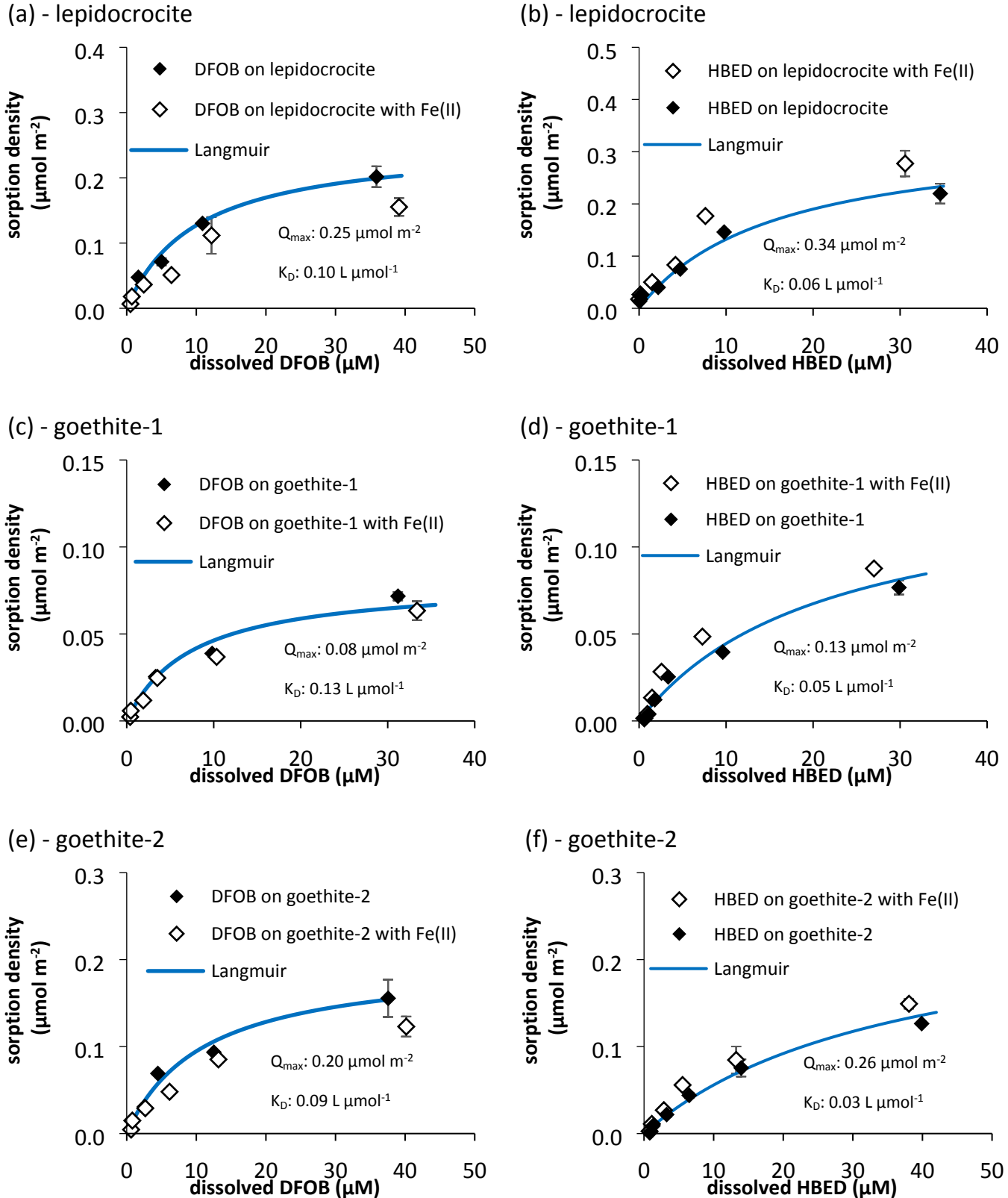
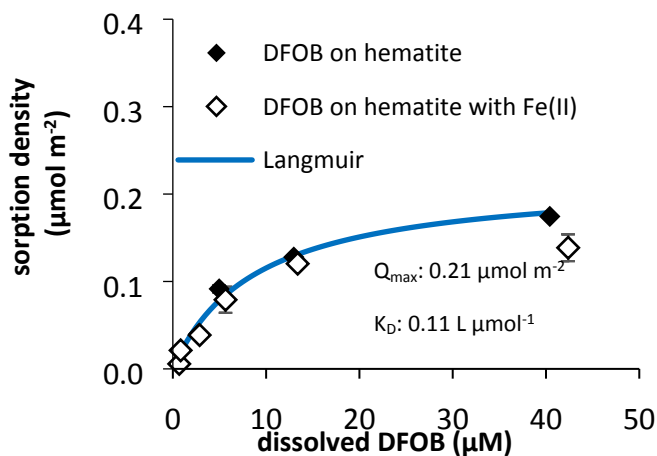


Figure. S2. Adsorption isotherms for DFOB and HBED onto various Fe(III) (hydr) oxide minerals (0.01 M NaCl) in the presence and absence of 1 μ M Fe(II) at pH 6. With lepidocrocite the equilibration time was 1 min for both DFOB and HBED, for goethite-1, goethite-2 and hematite it was 15 min for DFOB and 1 min for HBED. The suspension density was 1 g L⁻¹ for lepidocrocite and 2.5 g L⁻¹ for goethite-1 and -2 and hematite. Adsorption data were obtained for an applied ligand concentration range from 1 μ M to 50 μ M. For ligand adsorption in absence of Fe(II), data were fit using the Langmuir equation (blue line), and Q_{max} and K_D were determined.



(g) - hematite



(h) - hematite

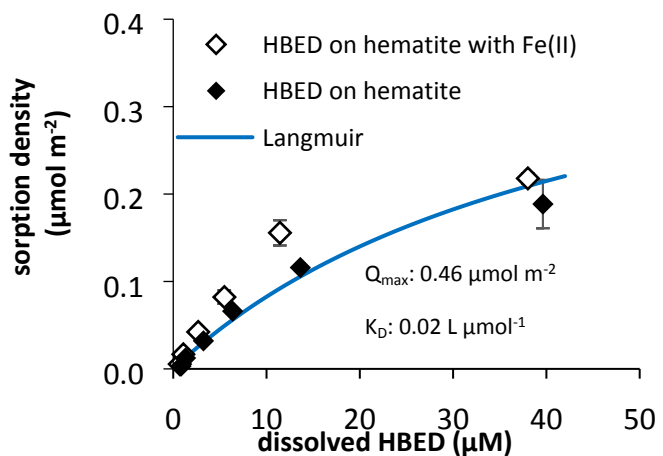
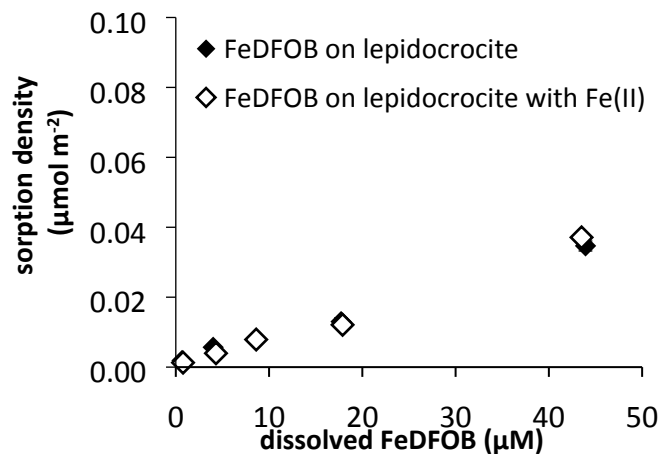
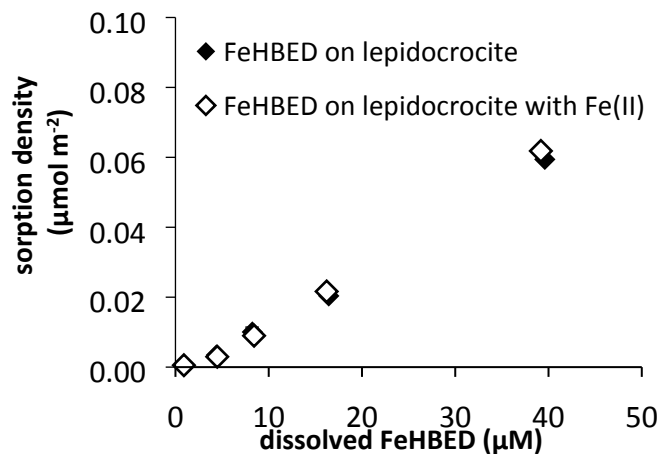


Figure. S3. Adsorption isotherms for Fe(III)DFOB and Fe(III)HBED onto (a-b) lepidocrocite and (c-d) goethite (0.01 M NaCl) in the presence and absence of 1 μ M Fe(II) at pH 6. The equilibration time was 30 minute. The suspension density was 2.5 g L⁻¹. Adsorption data were obtained for an applied ligand concentration range from 1 μ M to 50 μ M.

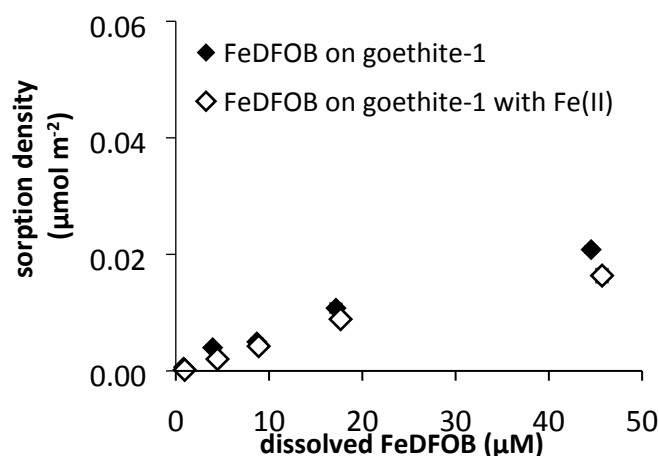
(a) - lepidocrocite



(b) - lepidocrocite



(c) - goethite-1



(d) - goethite-1

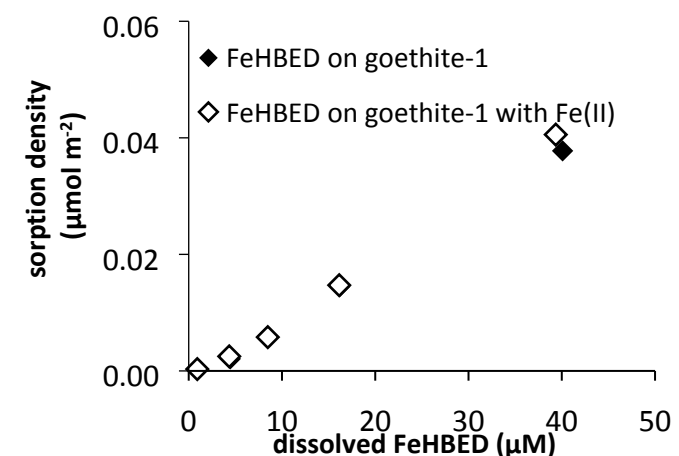
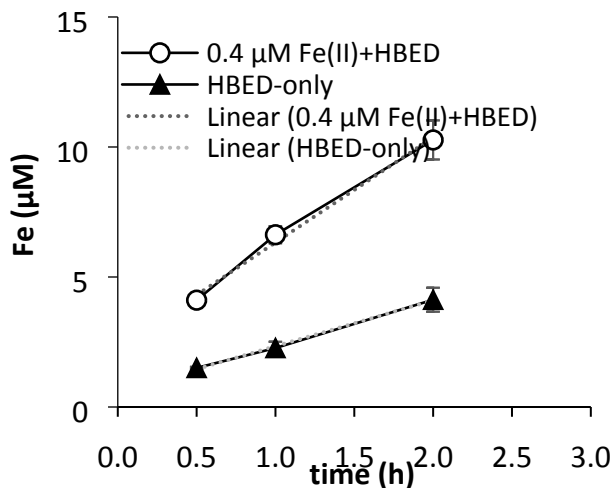
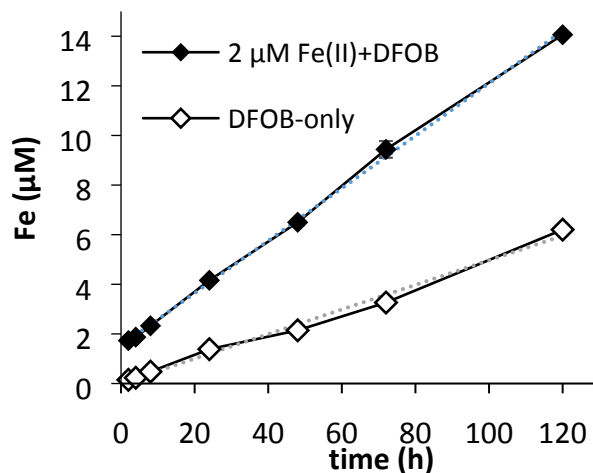


Figure. S4. Procedure for calculating the dissolution rates. Dissolution rates were calculated from the slopes of linear regression lines of the dissolved Fe concentrations over time for the initial linear part of data points; (a) three data points from most of treatments with lepidocrocite, (b) more than three points from the treatments with goethite-1, -2, hematite and 2-line ferrihydrite. Selected data points for each treatment were shown in Table. S2. (c) Calculated dissolution rates including mass- and surface area normalized rates.

(a)- lepidocrocite



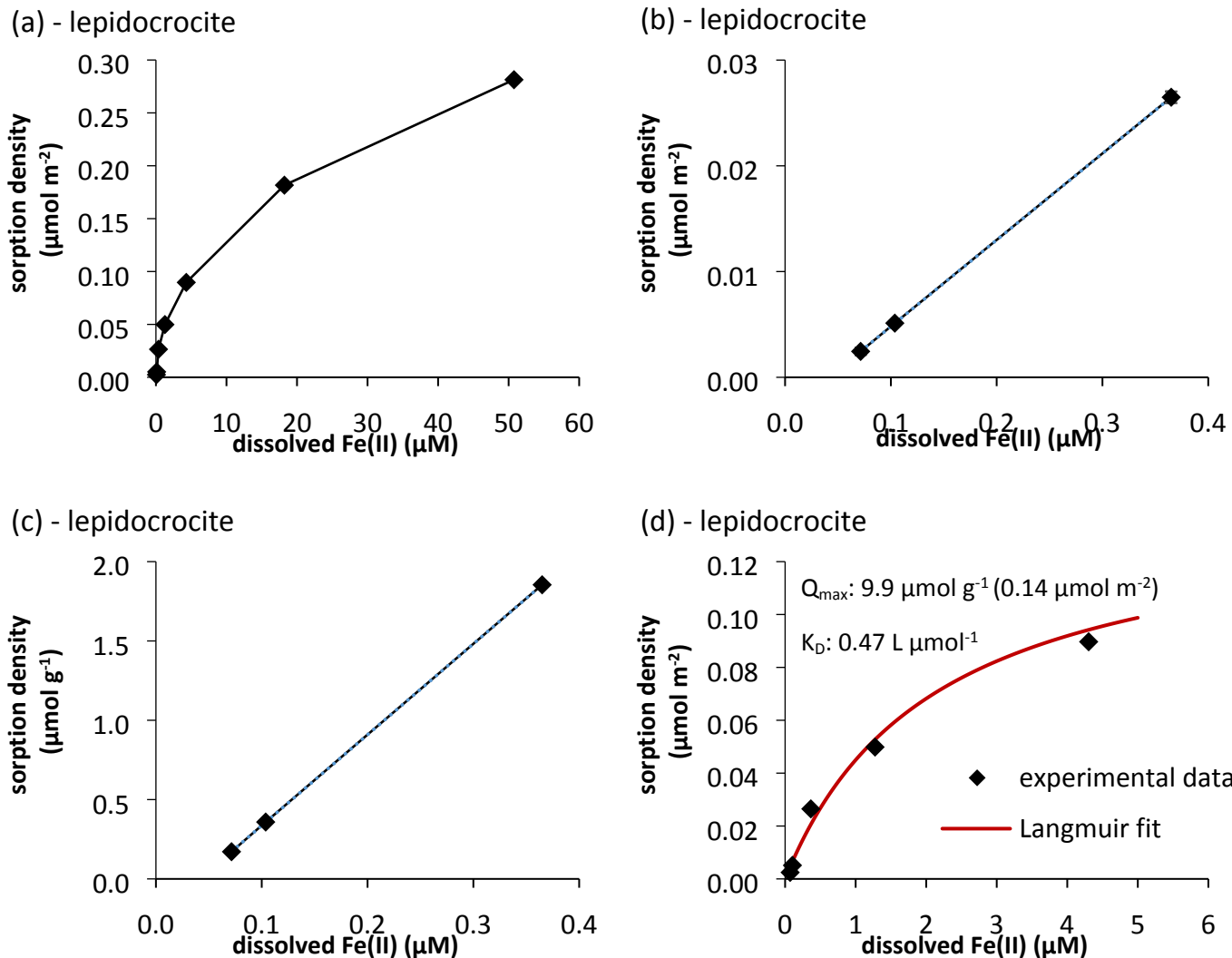
(b)-goethite-2



(c)- calculated rates

Treatment	μM h ⁻¹	μmol h ⁻¹ g ⁻¹	pmol sec ⁻¹ m ⁻²
lepidocrocite dissolution by 0.4 μM Fe(II) + HBED	4.0	40	1.6 · 10 ²
lepidocrocite dissolution by HBED	1.8	18	70
goethite-2 dissolution by 2 μM Fe(II) + DFOB	0.11	1.1	9.2

Figure. S5. Calculation of the adsorbed Fe(II) concentration in dissolution experiments ($SSR = 0.1 \text{ g L}^{-1}$) at $t=0$ using the adsorption isotherms; batch experimental data for adsorption of Fe(II) on lepidocrocite at pH 6 (a), linear part of the adsorption isotherm with different sorption density units (b): $\mu\text{mol m}^{-2}$ and (c) $\mu\text{mol g}^{-1}$, the Langmuir fit of the adsorption isotherm (d).



For the range of 0 to 0.4 μM dissolved Fe(II) concentrations, the adsorbed amount of Fe(II) onto Fe(III) (hydr) oxide minerals was calculated based on the linear part of Fe(II) adsorption isotherm using equations (S-1 and 2) from Schenkeveld et al., 2017.

$$C_{T(a)} = C_{L(a)} * (1 + \alpha * SSR_{(a)}) \quad \text{Equation (S-1)}$$

$$C_{L(batch)} = \frac{C_{T(batch)}}{(1 + \alpha * SSR_{(batch)})} \quad \text{Equation (S-2)}$$

$C_{T(a)}$: total Fe(II) concentration in suspension at the adsorption experiment ($\mu\text{mol L}^{-1}$), $C_{L(a)}$: the measured solution concentration at the adsorption experiment ($\mu\text{mol L}^{-1}$), $C_{T(batch)}$: total Fe(II) concentration in suspension at the batch dissolution experiment ($\mu\text{mol L}^{-1}$), $C_{L(batch)}$: the estimated solution concentration at

the bath dissolution experiment ($\mu\text{mol L}^{-1}$), α : slope of the linear adsorption isotherm (L g^{-1}), SSR: solid (Fe(III) (hydr)oxides) solution ratio (g L^{-1})

For the range of 0.5 to 5 μM dissolved Fe(II) concentrations, the adsorbed amount of Fe(II) onto Fe(III) (hydr) oxide mineral was calculated based on the Langmuir fit of Fe(II) adsorption isotherm using equations (S-3 and 4) from Schenkeveld et al., 2017.

$$C_{T(a)} = C_{L(a)} * \left(1 + \frac{Q_{max} * K_D * SSR_{(a)}}{1 + K_D * C_{L(a)}}\right)$$

Equation (S-3)

$$C_{L(batch)} = \frac{-(1 + K_D * (Q_{max} * SSR_{batch} - C_T)) + \sqrt{(1 + K_D * (Q_{max} * SSR_{batch} - C_T))^2 + 4 * K_D * C_{T(batch)}}}{2 * K_D}$$

Equation (S-4)

Q_{max} : the maximum adsorption in the Langmuir fit ($\mu\text{mol m}^{-2}$), K_D : the affinity constant of the Fe(II) for the Fe(III) (hydr) oxide mineral in the Langmuir fit ($\text{L } \mu\text{mol}^{-1}$),

Schenkeveld et al., 2017¹

Figure. S6. Rate coefficients for (a) ligand-controlled dissolution (k_{HBED}) and (b) Fe(II) catalyzed ligand-controlled dissolution ($k_{Fe(II)}HBED$) of various Fe(III) (hydr)oxide minerals by HBED.

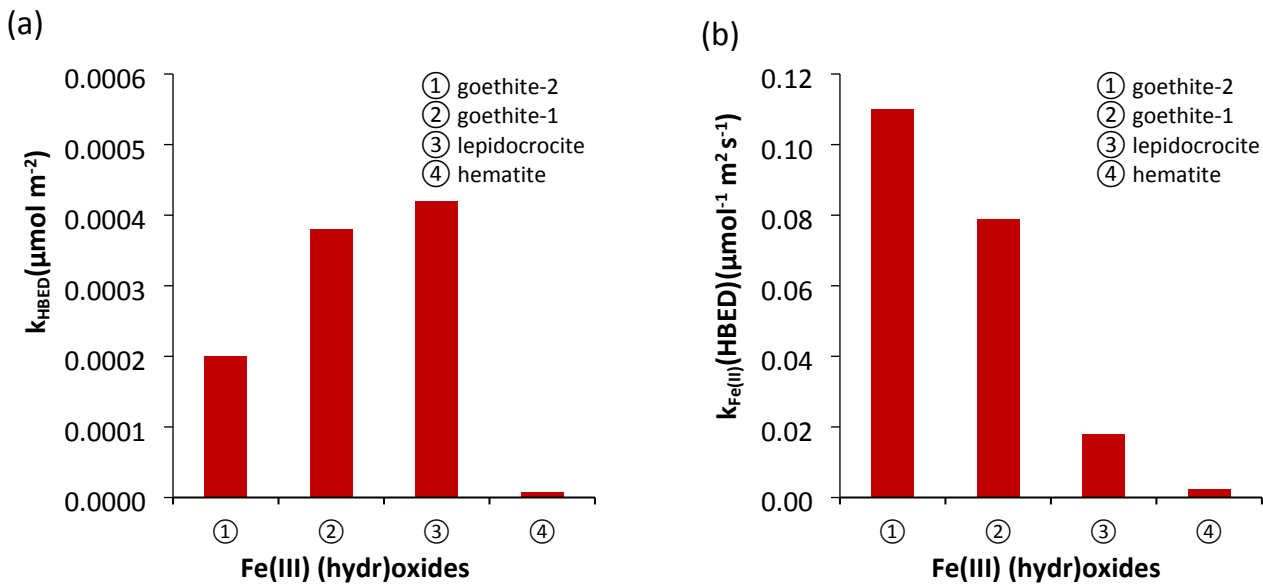
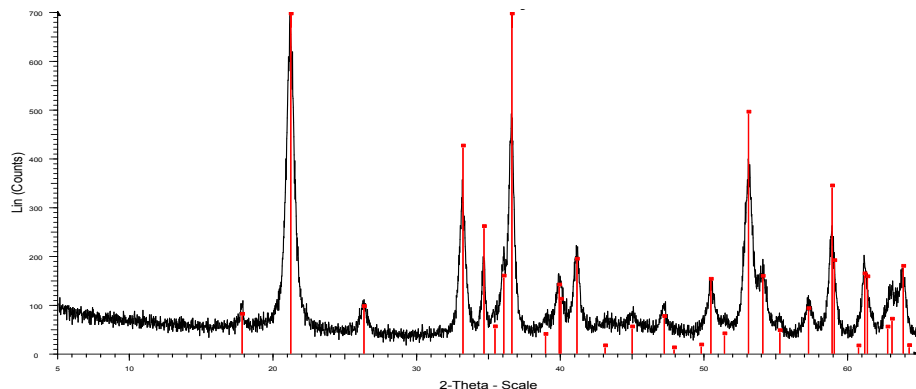
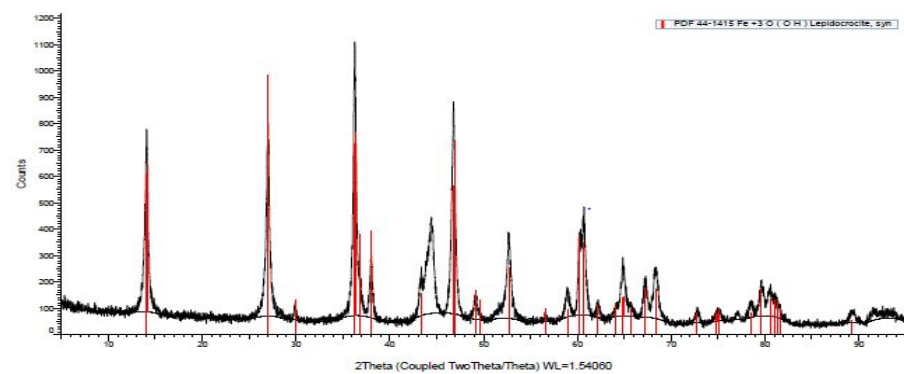


Figure. S7. XRD patterns of synthesized Fe(III) (hydr)oxides

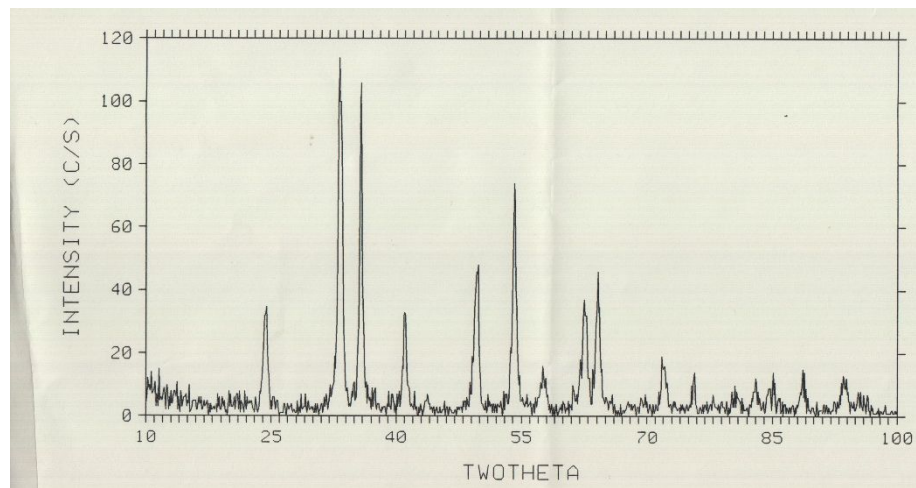
(a)-goethite-1



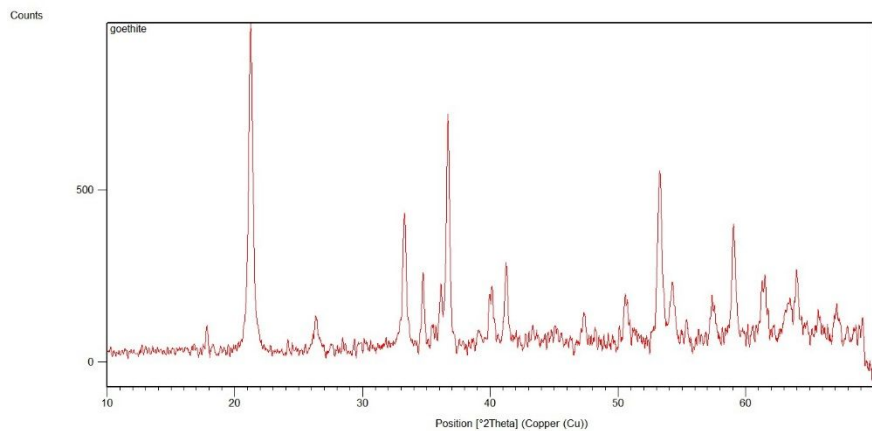
(b)-lepidocrocite



(c)- hematite



(d) goethite-2



(e) 2-line ferrihydrite (green line)

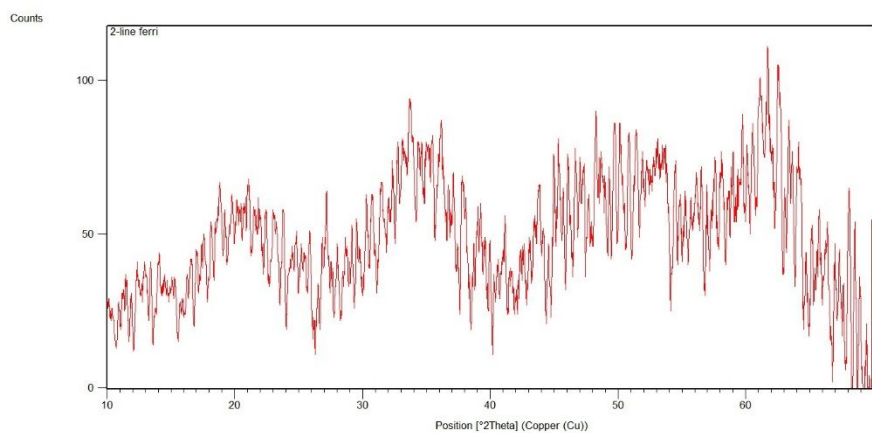


Table. S1. List of chemicals used for dissolution and adsorption experiments.

chemical	formula	supplier	purity	stock concentration (M)
mesylate salt of desferrioxamine B (DFOB)	C ₂₅ H ₄₈ N ₆ O ₈ ·CH ₄ O ₃ S	Novartis	>97%	8.0 × 10 ⁻⁴
<i>N,N'</i> -di(2-hydroxybenzyl)ethylene-diamine- <i>N,N'</i> -diacetic acid monohydrochloride hydrate (HBED)	C ₂₀ H ₂₄ N ₂ O ₆ ·HCl· H ₂ O	Strem Chemicals	>88%	7.0 × 10 ⁻⁴
Fe(II) chloride tetrahydrate	FeCl ₂ · 4H ₂ O	Merck	>99%	1.0 × 10 ⁻⁴
Fe(III) nitrate nonahydrate	FeN ₃ O ₉ · 9H ₂ O	Fisher chemical	>98%	1.0 × 10 ⁻¹
sodium hydroxide	NaOH	Merck	>99%	5.0 × 10 ⁻¹
sodium chloride	NaCl	Merck	>99.5%	2.0 × 10 ⁻¹
piperazine-1,4-bis-(propane-sulfonic acid) (PIPPS)	C ₁₀ H ₂₂ N ₂ O ₆ S ₂	Merck	>97%	1.0 × 10 ⁻¹
2-morpholinoethanesulfonic acid monohydrate (MES)	C ₆ H ₁₄ N ₂	Merck	>99%	1.0 × 10 ⁻¹
3-(<i>N</i> -morpholino)propanesulfonic acid (MOPS)	C ₇ H ₁₅ NO ₄ S	Carl Roth GmbH + Co	>99%	1.0 × 10 ⁻¹

Table. S2. Summary of batch experiments and dissolution rates. Surface normalized dissolution rates were calculated from the slopes of linear regression lines of the dissolved Fe concentration over time.

Fe(III) (hydr) oxide (SSR, g L ⁻¹)	pH	ligand (μM)	Fe(II) (μM)	dissolution rates (pmol s ⁻¹ m ⁻²)	linear regression line for data points
lepidocrocite (0.1)	6	HBED (17.6)	0	70	0.5 h – 2h
	6		0.1	88	0.5 h – 2 h
	6		0.2	94	0.5 h – 2 h
	6		0.4	1.6×10^2	0.5 h – 2 h
	6		0.6	1.9×10^2	0.5 h – 2 h
	6		0.8	-	0.5 h – 2 h
	6		1	-	0.5 h – 2 h
	6		5	-	0.5 h – 2 h
	6	DFOB (20)	0	42	0.5 h – 2 h
	6		0.5	54	0.5 h – 2 h
	6		1	55	0.5 h – 2 h
	6		2	68	0.5 h – 2 h
	6		5	1.8×10^2	5 min -30 min
	6		ª5	1.9×10^2	5 min -30 min
	4		0	24	2 h – 9 h
	4		5	27	2 h – 9 h
goethite-1 (0.1)	7	HBED (17.6)	0	68	0.5 h – 2 h
	7		0	73	1 min – 2h
	7	DFOB (20)	2	2.9×10^2	1 min – 30 min
	7		5	5.6×10^2	5 min -30 min
goethite-2 (0.1)	7	HBED (17.6)	ª 5	4.6×10^2	5 min -30 min
	8.5		0	69	0.5 h – 2 h
	8.5	DFOB (20)	5	2.7×10^2	5 min -30 min
	8.5		ª 5	2.5×10^2	5 min -30 min
hematite (0.1)	6	HBED (17.6)	0	24	0.5 h – 8 h
	6		1	1.9×10^2	1 min – 1 h
	7	DFOB (20)	0	1.8	0.5 h – 72 h
	7		2	3.2	0.5 h – 72 h
2-line ferrihydrite (0.1)	6	HBED (17.6)	0	18	0.5 h – 24 h
	6		1	2.3×10^2	10 min to 2 h
	7	DFOB (20)	0	4.3	2 h – 120 h
	7		2	9.2	2 h – 120 h
	6	HBED (17.6)	0	8.5×10^{-1}	8 h -120 h
	6		1	5.9	8 h -120 h
	7	DFOB (20)	0	4.5×10^{-1}	8 h -168 h
	7		2	9.5×10^{-1}	8 h -168 h
	6	HBED (17.6)	0	ª 3.4×10^3	1 min to 4 h
	6		1	ª 1.0×10^4	1 min to 4 h
	7	DFOB (20)	0	ª 1.2×10^3	1 min to 4 h
	7		2	ª 4.9×10^3	1 min to 2 h

ª Addition of Fe(II) and DFOB at the same time. ª unit of 2-line ferrihydrite dissolution rates is pmol s⁻¹ g⁻¹ (normalized by mass (g) not specific surface area), because ligand-accessible specific surface area cannot be determined by BET analysis.

Table S3: Percentage of 5 µM Fe(II) complexed by 20 µM DFOB at I = 0.01 M (10 mM NaCl), in absence of surfaces, as modelled for equilibrium conditions with PhreeqC using the Minteq v4 database² supplemented with protonation and complexation constants for DFOB presented in Kim et al³.

pH	percentage of Fe(II) complexed by DFOB (%)
6	<1
7	42
8.5	100

Table. S4. Effect of pH on the catalytic effect (C.E.) of 5 μM Fe(II) on the ligand-controlled lepidocrocite dissolution rate in the presence of 20 μM DFOB. Fe(II) was added to the suspension either (a) 20 minutes before addition of the ligand or (b) at the same time as the ligand. Surface normalized dissolution rates were calculated from the slopes of linear regression lines of the dissolved Fe concentration. The catalytic effect is the ratio of dissolution rates in the presence and the absence of Fe(II). Listed $\text{Fe}(\text{II})_{\text{ads}}$ concentrations are based on $\text{Fe}(\text{II})$ adsorption isotherm data in absence of DFOB (Figure S1 a&b).

	R_{DFOB} (pmol $\text{s}^{-1} \text{m}^{-2}$)	$\text{Fe}(\text{II})_{\text{ads}}$ ($\mu\text{mol m}^{-2}$)	$R_{\text{Fe}(\text{II})(20 \text{ min earlier})+\text{DFOB}}^{\text{a}}$ (pmol $\text{s}^{-1} \text{m}^{-2}$)	$R_{\text{Fe}(\text{II})+\text{DFOB}}^{\text{b}}$ (pmol $\text{s}^{-1} \text{m}^{-2}$)	C.E. $\text{Fe}(\text{II})$ (from a)	C.E. $\text{Fe}(\text{II})$ (from b)
pH 4	24	8.6×10^{-3}	27		1.1	
pH 6	42	4.2×10^{-1}	1.9×10^2	1.8×10^2	4.6	4.2
pH 7	73	6.0×10^{-1}	5.6×10^2	4.6×10^2	7.6	6.3
pH 8.5	69	6.6×10^{-1}	2.7×10^2	2.5×10^2	4.0	3.7

1. Schenkeveld, W. D. C.; Kimber, R. L.; Walter, M.; Oburger, E.; Puschenreiter, M.; Kraemer, S. M., Experimental considerations in metal mobilization from soil by chelating ligands: The influence of soil-solution ratio and pre-equilibration - A case study on Fe acquisition by phytosiderophores. *Sci. Total Environ.* **2017**, *579*, 1831-1842.
2. Parkhurst, D. L. a. A., C. A. *Description of input and examples for PHREEQC Version 3 – a computer program for speciation, batch-reaction, onedimensional transport and inverse geochemical calculations.*; 2013; p 497.
3. Kim, D.; Duckworth, O. W.; Strathmann, T. J., Reactions of aqueous iron-DFOB (desferrioxamine B) complexes with flavin mononucleotide in the absence of strong iron(II) chelators. *Geochim. Cosmochim. Acta* **2010**, *74*, (5), 1513-1529.